AIAA-2001-3677

Alleviation of Facility/Engine Interactions in an Open-Jet Scramjet Test Facility

C.W. Albertson
NASA Langley Research Center
Hampton, VA

S. Emami
Lockheed Martin Engineering and Science Company
Hampton, VA

37th Joint Propulsion Conference & Exhibit
8-11 July 2001
Salt Lake City, Utah

ALLEVIATION OF FACILITY/ENGINE INTERACTIONS IN AN OPEN-JET SCRAMJET TEST FACILITY

Cindy W. Albertson*
NASA-Langley Research Center
Hampton, Virginia 23681-2199

Saied Emami†
Lockheed Martin Engineering and Science Company
Hampton, Virginia 23681-2199

Abstract

Results of a series of shakedown tests to eliminate facility/engine interactions in an open-jet scramjet test facility are presented. The tests were conducted with the NASA DFX (Dual-Fuel eXperimental scramjet) engine in the NASA Langley Combustion Heated Scramjet Test Facility (CHSTF) in support of the Hyper-X program. The majority of the tests were conducted at a total enthalpy and pressure corresponding to Mach 5 flight at a dynamic pressure of 734 psf. The DFX is the largest engine ever tested in the CHSTF. Blockage, in terms of the projected engine area relative to the nozzle exit area, is 81% with the engine forebody leading edge aligned with the upper edge of the facility nozzle such that it ingests the nozzle boundary layer. The blockage increases to 95% with the engine forebody leading edge positioned 2 in. down in the core flow. Previous engines successfully tested in the CHSTF have had blockages of no more than 51%. Oil flow studies along with facility and engine pressure measurements were used to define flow behavior. These results guided modifications to existing aeroappliances and the design of new aeroappliances. These changes allowed fueled tests to be conducted without facility interaction effects in the data with the engine forebody leading edge positioned to ingest the facility nozzle boundary layer. Interaction effects were also reduced for tests with the engine forebody leading edge positioned 2 in. into the core flow, however some interaction effects were still evident in the engine data. A new shroud and diffuser have been designed with the goal of allowing fueled tests to be conducted with the engine forebody leading edge positioned in the core without facility interaction effects in the data. Evaluation tests of the new shroud and diffuser will be conducted once ongoing fueled engine tests have been completed.

Introduction

Propulsion testing of the Mach 5 DFX (Dual-Fuel eXperimental scramjet) engine is ongoing in NASA Langley's Combustion Heated Scramjet Test Facility (CHSTF) in support of Mach 5 flowpath development for NASA's Hyper-X program. Although the Mach 5 flight test has been eliminated from the Hyper-X program, Mach 5 ground tests continue for the purpose of technology development. One of the primary purposes of the present test series is to provide a database to directly compare engine performance and operability between two types of facilities commonly used for scramjet propulsion research. Tests were initially conducted in the NASA Langley Arc Heated Scramjet Test Facility (AHSTF), which has a test gas composition close to air (ref. 1). These tests were conducted at a total enthalpy and pressure corresponding to Mach 5 flight at a dynamic pressure of 885 psf. In

*Aerospace Research Engineer, Hypersonic Airbreathing Propulsion Branch
†Principal Engineer, Assigned to the Hypersonic Airbreathing Propulsion Branch

order to obtain as good a comparison as reasonably possible, the same engine hardware and force balance that were tested in the AHSTF were then installed in the CHSTF. However, due to facility interaction problems encountered in the past with large blockage engines, it was recognized that a series of shakedown tests would be necessary in order to minimize interactions between the facility and engine. The steps taken to minimize interaction effects in the CHSTF are the subject of this paper.

The DFX is the largest engine ever tested in the CHSTF. Blockage, in terms of the projected engine area (including interior flowpath area) relative to the nozzle exit area, is 81% with engine cowl closed and with the engine forebody leading edge aligned with the upper edge of the facility nozzle such that it ingests the nozzle boundary layer. The blockage increases to 95% with the engine forebody leading edge positioned 2 in. down in the core flow. Previous engines successfully tested in this facility have had blockages of no more than 51%.

The shakedown tests described in this report were primarily conducted at a total enthalpy and pressure corresponding to Mach 5 flight at a dynamic pressure of 734 psf. The dynamic pressure was reduced from the dynamic pressure of the AHSTF tests because of concerns that the interaction loads at the higher pressure could exceed the force balance design loads. Oil flow studies along with facility and engine pressure measurements were used to define flow behavior. These results guided modifications to existing aeroappliances and the design of new aeroappliances.

Nomenclature

h	diffuser duct height
m	facility total mass flow rate
p	pressure
q	dynamic pressure
x	axial distance
y	vertical distance
Ar	argon
H	enthalpy
H_2	hydrogen
H_2O	water vapor
M	Mach number
N_2	nitrogen
O_2	oxygen
T	temperature
ϕ	fuel equivalence ratio

Subscripts

ba	base of engine
c	test cabin
e	facility nozzle exit
e,d	design condition at facility nozzle exit
e,eng	engine nozzle exit
eng	engine
le	engine forebody leading edge
n	facility nozzle
t,h	total condition in the facility heater
t,2	total condition behind a normal shock
SiH_4	silane mixture (20% SiH_4, 80% H_2, by volumn)
∞	static condition upstream of aircraft bow shock

Description of Experiment

Test Facility

The CHSTF has been in operation since 1978 and has historically been used to test complete (inlet, combustor, and partial nozzle) subscale scramjet component integration models. To date, nearly 2000 tests have been conducted with a variety of engines including the NASA-Langley 3-Strut, NASA-Langley Step Strut, NASA-Langley Parametric, NASP Government Baseline, Rocketdyne A2, Pratt & Whitney C, JHU/APL B1, Rocketdyne A3 Hydrocarbon-Fueled Scramjet, and most recently, the NASA-Langley DFX engine under the Hyper-X program.

The CHSTF (shown schematically in figure 1) can operate at stagnation enthalpies duplicating that of flight at Mach numbers ranging from 3.5 to 6.0. These enthalpy levels are obtained by burning hydrogen and air in the facility heater. Oxygen is added upstream of the heater such that the oxygen content of final test gas matches that of air. Currently, either a Mach 3.5 or 4.7 nozzle may be installed between the heater and test cabin to expand the test gas to the desired conditions. Both nozzles are a two piece design (throat and expansion sections), have square cross sections, and are contoured to exit dimensions of 13.26 by 13.26 in. In addition to exit Mach number, the main difference between the two nozzles is that the M3.5 nozzle is a heat sink design, while the M4.7 nozzle is water-cooled in the throat section and along a portion of the expansion section. For the present tests series,

the Mach 4.7 nozzle was used. This nozzle is relatively new and has just undergone a series of calibration tests. The nozzle flow exhausts into the test cabin, which has interior dimensions of 42 in. high by 30 in. wide by 96 in. long. The jet from the nozzle passes through and around the engine model and then into the facility diffuser. The flow is typically exhausted into a 70-ft. vacuum sphere. (The air ejector shown in fig. 1 is no longer used.)

The facility is typically operated such that flow conditions at the engine inlet entrance plane are matched with that of the flight vehicle (fig. 2). To accomplish this, the facility heater is operated at the flight total enthalpy, which is constant across the bow shock, and the flow in the facility nozzle is expanded to conditions matching those at the vehicle engine inlet entrance plane. The facility normally operates at heater stagnation pressures between 50 and 500 psia and at stagnation temperatures between 1300 and 3000 °R. The flight dynamic pressure ranges from 250 to 3500 psf, depending on Mach number. Test gas mass flow rates range from 10 to 60 lbm/s. The range of operation is shown by the Mach number and altitude simulation envelope (fig. 3). The left vertical boundary of the envelope is the nozzle exit Mach number of 3.5 and the right vertical boundary reflects the maximum heater operating temperature of 3000 °R. The upper inclined boundary represents the minimum operating pressure of 50 psia, up to an altitude where a flight dynamic pressure of 250 psf is imposed as a limit. The lower inclined boundary reflects the maximum mass flow rate to the heater at the Mach number of 3.5 limit and the maximum heater operating pressure at the Mach number of 6 limit. Calculated test gas compositions for these conditions are shown in figure 4. The primary contaminant in the test gas is water vapor, which varies from 0.060 mole fraction at Mach 3.5 to 0.198 at Mach 6.0.

The facility currently has a gaseous engine fuel system consisting of six independently controlled fuel circuits which can be connected to any combination of injection stations in the engine. One circuit supplies a pyrophoric mixture of silane and hydrogen (20 percent silane and 80 percent hydrogen, by volume) for igniting and piloting the fuel. Gaseous hydrogen and ethylene have been used as the primary fuel in past engine tests.

Additional details of the CHSTF are given in refs. 2 – 4.

Data Acquisition, Instrumentation, and Flow Visualization

The data acquisition system (DAS) consists of a commercially available software package (AutoNet) running on a Pentium processor. The DAS incorporates a NEFF 300 signal conditioner and a NEFF 600 amplifier/ multiplexer capable of supporting 128 channels of instrumentation. In addition, up to 512 pressure measurements can be recorded using a PSI 8400 ESP system and sixteen 32-port modules.

In addition to the standard instrumentation for health monitoring and defining flow conditions, instrumentation is also provided to assist in assessing engine/facility interaction effects. This instrumentation primarily consists of static pressure measurements located along the facility nozzle, inside the test cabin, at the base of the DFX engine, and along the facility diffuser (fig. 5). Pitot probes are located at the facility mixer entrance and exit. A single total temperature probe is located at the mixer entrance.

Oil flow studies were conducted during this investigation to define flow behavior and to aid in locating flow fences and other modifications. The oil flow mixture consisted of a mixture of 50% (by volume) of 80W-140 gear oil and 50% of a commercially available oil thickener manufactured for automobile engines. Lampblack was added to the mixture to provide visibility.

Model and Installation

The engine was installed in the CHSTF test cabin as illustrated in figure 6. The engine and force balance were mounted at the top of the test cabin through a series of attachments as shown. Initially the forebody leading edge of the engine was positioned 2.0 inches below the upper wall of the nozzle at the exit plane (y_{le} = 2.0 in.). This position was chosen to match the engine position for the majority of the runs from the AHSTF tests. The angle of the engine relative to the facility nozzle water line was adjusted such that the Mach number just ahead of the cowl leading edge matched that measured during the Mach 5 DFX tests in the AHSTF.

The initial aeroappliances consisted of the same nozzle extension skirt and catch cone diffuser used successfully with previous tests of lower blockage engines. The purpose of the nozzle extension skirt is to position the Mach wave from the nozzle exhaust far enough downstream that it doesn't disturb the flow delivered to the engine inlet. The catch cone

catches the nozzle exhaust and directs it into the diffuser. A washer (fig. 7) is located at the entrance of the catch cone to prevent any separated flow on the wall of the catch cone from spilling out into the test cabin. The washer also restricts the area around the engine at the catch cone entrance and enhances the aspiration of the test cabin. Water is injected parallel to the flow near the engine nozzle exit to reduce the temperature and associated pressure rise from the engine exhaust and test gas. This lessens the probability of facility interference with the force balance measurements and engine nozzle pressures.

As shown in figure 6, the DFX engine incorporates a cowl that rotates about a point near the cowl leading edge, allowing the contraction ratio to be reduced to allow the engine to start. Figure 6 shows the cowl open at the 12° position as was used during the AHSTF tests. As discussed in the Results and Discussion section, it was found that this angle could be reduced significantly while still enabling the engine to start.

Test Conditions and Procedure

The first set of tests was conducted at a reduced stagnation pressure and temperature of 100 psia and 1600°R, respectively, to minimize loads on the force balance while determining the maximum load level from facility start-up to shut-down. Tests continued at this condition to determine the minimum cowl-open angle necessary to start the engine.

Follow-on tests were primarily conducted at a Mach 5 flight enthalpy to match the bulk of the Mach 5 DFX tests in the AHSTF. The total temperature corresponding to this enthalpy level was 2095 °R for the vitiated test gas. The nominal total pressure in the facility heater was reduced to 175 psia compared to 210 psia for the AHSTF tests to minimize loads on the force balance due to facility interactions. The corresponding flight dynamic pressure was 734 psf compared to 885 psf for the AHSTF tests. The nominal test conditions and test gas mole fractions are summarized in tables 1 and 2, respectively. The test gas mole fractions were calculated assuming complete combustion of the hydrogen and frozen flow along the facility nozzle.

A typical test sequence is illustrated in fig. 8. First the tunnel air flow is established (10 to 60 lb/sec.). The heater ignitor is then activated and once good ignitor operation is verified, the timer reset circuit is energized, initiating the opening of the vacuum valve. Hydrogen is then allowed to flow into the facility heater, increasing the temperature and pressure. Once good combustion in the heater is established, the timer start circuit is activated, allowing oxygen to be added upstream of the heater (See fig. 1). Facility steady-state flow conditions are obtained in about 5 seconds, which is considered the no-fuel tare data point. At 6 seconds into the run, the model fuel sequence is initiated. Tests are terminated automatically by the run timer (typically 20 seconds).

Results and Discussion

Baseline Configuration and Modifications, y_{le} = 2.0 in.

Tests were initially conducted without engine fuel and with the baseline configuration at the y_{le} = 2.0 in. position in the facility (figs. 6 and 7). The first set of tests were conducted at a reduced stagnation pressure and temperature of 100 psia and 1600°R, respectively, to minimize loads on the force balance while determining the maximum load level from facility start-up to shut-down. Tests continued at this condition to determine the minimum cowl-open angle necessary to start the engine. Results showed that a cowl-open angle of approximately 3° was sufficient for starting the inlet. The timing of the cowl closing was then optimized to minimize loads on the force balance while obtaining a started inlet. Results showed that the cowl could be closed about 2 seconds after the facility vacuum valve opened (fig. 8) while the heater pressure was still increasing.

Follow-on tests to minimize facility/engine interactions were conducted at the nominal condition of $p_{t,h}$ = 175 psia and $T_{t,h}$ = 2095°R. The pressures measured along the facility nozzle wall for the baseline configuration (fig. 9) were high and exceeded the predicted value near the nozzle exit by a factor of 2.69 (table 3). Predictions were based on three-dimensional full Navier Stokes calculations assuming frozen flow down the nozzle length (ref. 5). The measured cabin pressure was a factor of 1.97 higher than the measured nozzle exit pressure (table 3) and 5.30 higher than the predicted static pressure at the nozzle exit. Apparently, the cabin pressure was high enough to feed forward along the facility nozzle wall and separate the boundary layer.

The sidewalls of the nozzle extension skirt were then modified (fig. 10) to eliminate the shock

losses and associated drag caused by its close lateral proximity (1.5 in.) to the engine forebody fences. As a result, the overall level of the nozzle pressure distribution decreased to nearly that of the CFD prediction (fig. 9). However, the test cabin pressure was a factor of 3.11 higher than the measured nozzle exit pressure (table 3), which is still high enough to cause boundary-layer separation. Oil flow obtained on the nozzle extension skirt show some turning of the flow, probably as a result of the high cabin pressure feeding forward along the corners of the skirt (fig. 11). Oil flow patterns obtained on the catch cone top cover extension plate and catch cone washer (fig. 12) indicate that some of the flow was spilled into the test cabin. The diffuser distributions given in fig. 13 show a significant pressure drop with the nozzle skirt modification. Also, pitot pressures obtained at the exit of the 19-in. diameter duct decreased with the nozzle skirt modification (fig. 14), reflecting higher Mach numbers at this station. In spite of the drop in static pressures in the exhaust duct, the engine pressure distributions still showed signs of boundary-layer separation near the engine nozzle exit. This indicated that the pressures in the catch cone and 19 in. duct were high enough to feed forward into the engine nozzle.

In an attempt to better direct the flow into the catch cone, flow fences were added to the catch cone top cover extension plate (fig 15). In spite of this modification, the test cabin pressure was still high at 3.16 times the measured nozzle exit pressure (table 3). Only slight changes were noted in the nozzle pressure distribution (fig. 9), the diffuser pressure distribution (fig. 13) and the pitot pressure distribution (fig. 14) with the addition of the flow fences. The engine pressure distributions improved slightly because of lower base pressure (table 3), but still showed signs of boundary-layer separation. Because of this, the fuel-off force measurement was unreliable. Therefore, it was decided not to attempt to fuel the engine at the y_{le} = 2.0 in. position with the current diffuser and catch cone design.

Modified Configuration, y_{le} = 0.0 in.

The engine was then raised out of the core such that the forebody leading edge was level with the nozzle exit (y_{le} = 0.0 in.) (See fig. 16.) This reduced the blockage from 95% to 81% with the cowl in the closed position. No additional changes were made to any of the areoappliances. The cabin pressure was reduced to approximately twice the nozzle exit pressure, as indicated by the static pressure distribution along the facility nozzle wall shown in fig. 17 and in table 3. Pressure distributions along the facility diffuser are also noticeably lower (fig. 18.), as were the pitot distributions at the end of the 19 in. dia. duct (fig. 19). Pressures on the engine forebody and nozzle showed no indication of interactions with the facility.

Based on these results, a fueled run was attempted. A plot showing various pressures as a function of time for the current test configuration is shown in figure 20. The data, taken at 20 Hz, show that the inlet unstarted at 21.1 sec. into the run while the fuel flow rate to the engine combustor was slowly increasing. The engine base pressure increased about the same time. However, the facility diffuser, cabin, and nozzle exit pressures were not affected until about 0.15 seconds later. These results indicate that the DFX engine can be successfully tested up to the point of inlet unstart without facility interaction effects at the y_{le} = 0.0 in. engine position in the test cabin.

Facility Diffuser Modifications

Various sources were consulted in the redesign effort of the catch cone and diffuser. Unfortunately, the actual flow within these components is complicated by three-dimensional interactions of shock waves and boundary layers. The flow is further complicated with the addition of a geometrically complex engine and its exhaust. Because of the flow complexity and unknowns, one must resort to empirically based guidelines.

Literature Guidelines

There are a number of reports describing various guidelines in designing supersonic diffusers as summarized in refs. 6 and 7. Many of the reports listed in these summaries were written in the 1960's and earlier. Of particular interest for the present application are those that include blockage effects in facilities in which the model is fixed (as opposed to injected) in the flow. Smaller diffuser diameters tend to be more efficient, however, one must be careful not to overcontract the flow. The first-order approximation of Kantrowitz (ref. 8) is often used to provide a conservative estimate for the maximum geometric contraction ratio that permits supersonic flow. Other guidelines include length/ diameter recommendations for the second minimum to provide good isolation and corresponding run time

(ref. 6). One especially useful recommendation is to incorporate a rearward-facing step in the design to help isolate the flow in the vicinity of the test article from the sphere pressure.

The design of catch cones and shrouds to direct the flow into the diffuser is discussed in refs. 7 and 9. Aerodynamic tailoring of shroud surfaces is discussed in ref. 9.

The Redesigned Diffuser

The objective of the new diffuser design is to reduce the losses to the flow and associated effects in the engine data, without compromising run time and also without having to replace any more components than necessary. The catch cone and 19 in. I.D. (inside diameter) constant area diffuser were targeted for redesign, based on the relatively high wall pressures measured in these areas (fig. 18). Other components that will be replaced include the original transition section, expansion bellows, and a small spool piece from the 25.25 in. I.D. dia. constant area section (fig. 21). The air ejector is no longer used and will be removed.

The strongest shock from the engine originates from the leading edge of the engine cowl. The resulting two-dimensional shock pattern is illustrated in figure 22 for the original catch cone configuration. A new shroud is being designed to replace the original catch cone (fig. 23). This shroud will be aerodynamically tailored to reduce the shock losses and will also have rectangular, as opposed to circular cross sections, consistent with the engine exterior geometry. This shroud will attach to a square-to-round contraction section that will fit into the transition section, as illustrated in figure 24. Water injectors will be incorporated into the new shroud to reduce the temperature and associated pressure rise from the engine exhaust and test gas.

The 19 in. I.D. constant area diffuser duct, which forms the second minimum, will be replaced with a 23.25 in I.D. constant area section (fig. 24). This cross-sectional area of the 23.25 in I.D. section is 50% larger than the original 19 in. I.D. section. This reduces the "duct blockage" (projected engine area/ second minimum area) from 50% to 34% with the engine positioned at y_{le} = 0.0 in. (engine cowl in closed position) and from 59% to 40% with the engine at y_{le} = 2.0 in. The 23.25 in. I.D. duct slides into the existing 25.25 in I.D. duct, resulting in a rearward facing step with overlap to provide isolation as the sphere pressure increases during the run. This sliding arrangement also allows for thermal expansion, eliminating the need for a new and larger bellows section, and also provides a length adjustment. This length adjustment eliminates the need for separate spoolpieces to accommodate the two different facility nozzles. A sliding seal is installed at the face of the flange attached to the 25.25 in. I.D. duct to minimize leaks.

The new diffuser components have been designed and constructed. The new shroud will be constructed and fitted in place following the completion of the DFX test series at the y_{le} = 0.0 in. location. Once all the new components are installed, some tests will be repeated with the DFX engine at y_{le} = 0.0 in. for comparison purposes. Tests will then be conducted with the engine lowered into the core flow at y_{le} = 2.0 in.

Concluding Remarks

A series of shakedown tests to eliminate facility/engine interactions in an open-jet scramjet test facility have been conducted. The tests were conducted with the NASA DFX (Dual-Fuel eXperimental scramjet) engine in the NASA Langley Combustion Heated Scramjet Test Facility (CHSTF) in support of the Hyper-X program. Oil flow studies along with facility and engine pressure measurements were used to define flow behavior. These results guided modifications to existing aeroappliances and the design of new aeroappliences. As a result of these changes, fueled tests could be conducted without facility interaction effects in the data with the engine forebody leading edge aligned with the upper edge of the facility nozzle such that it ingested the nozzle boundary layer. Interaction effects were reduced for tests with the engine forebody leading edge positioned 2 in. outside of the facility nozzle boundary layer, however some effects were still evident in the engine data. A new shroud and diffuser have been designed with the goal of further reducing blockage effects and allowing fueled tests to be conducted with the forebody leading edge of the engine positioned 2 in. into the core flow. Installation and evaluation of the new shroud and diffuser will commence once ongoing engine tests have been completed.

Acknowledgements

A special thanks to Bobby Huffman, Barry Lawhorne, and Clint Reese for their help with the model and instrumentation and also with the operation, diagnostics and repairs of the facility. Thanks to Don Harper for his help with all things that are DAS related, to Carl Davis for helping with the instrumentation and diagnostics, to Earl Andrews for his helpful suggestions and schematics relating to the new diffuser design, to Troy Middleton for initiating the detailed design and construction of the new diffuser, and to our new facility safety head, Diego Capriotti, for his facility help and also for his help with the DAS post-processing Fortran codes. Thanks also to Roger Jones for his help with many of the figures (plus revisions) contained within this report.

M_∞	$P_{t,h}$	$H_{t,h}$	$T_{t,h}$	q_∞	M_n	m
	(psia)	(Btu/ lbm)	°R			lbm/s
5.0	175	573	2095	734	4.7	12.3

Table 1. Nominal test condition for the present series of shakedown tests.

M_∞	N_2	O_2	H_2O	Ar
5.0	.6477	.2095	.1338	.0090

Table 2. Test gas mole fractions at the nominal test condition given in table 1.

References

1. Guy, R. W.; Rogers, R. C.; Puster, R. L.; Rock, K. E.; Diskin, G. S.: The NASA Langley Scramjet Test Complex. AIAA-96-3243, July 1996.
2. Andrews, Earl H., Jr.; Torrence, Marvin G.; Anderson, Griffin Y.; Northam, G. Burton; and Mackley, Earnest A.: Langley Mach 4 Scramjet Test Facility. NASA TM-86277, 1985.
3. Andrews, Earl H., Jr.: A Subsonic to Mach 5.5 Subscale Engine Test Facility. AIAA-87-2052, June 1987.
4. Rock, Kenneth E.; Andrews, Earl H.; and Eggers, James M.: Enhanced Capability of the Combustion-Heated Scramjet Test Facility. AIAA-91-2502, June 1991.
5. Gaffney, Richard L., Jr.: Private communications with Richard L. Gaffney, Jr. Aerodynamics, Aerothermodynamics, and Acoustics Competency, NASA Langley Research Center, 2001.
6. Handbook of Supersonic Aerodynamics, Section 17, Ducts, nozzles and Diffusers. NAVWEPS Report 1488, January, 1964.
7. Andrews, Earl H., Jr.: Nozzle/Tunnel Starting in Free-Jet Engine Test Facilities. CPIA Publication 585, June 1994.
8. Kantrowitz, Authur and Donaldson, Coleman duP.: Preliminary Investigation of Supersonic Diffusers. NACA WR L-713, 1945.
9. Bulman, M.; Leonard, J.; Keenan, R.; and Wade, M. T.: Advancing the State of the Art in Hypersonic Testing; HYTEST/MTMI. AIAA Paper 93-2023.

Configuration	y_{le}	$p_e/p_{e,d}$	p_c/p_e	$p_{ba}/p_{e,eng}$	Facility/engine interactions?	
	(in.)				Forebody	Engine nozzle
Original (U*)	2.0	2.69	1.97	1.16	Yes	Yes
Modified skirt (U)	2.0	1.07	3.11	2.27	Yes	Yes
Modified skirt	2.0	1.07	3.16	1.28	No	Yes
+ fences (U)						
Modified skirt	0.0	1.07	2.28	1.20	No	No
+ fences (U)						
Modified skirt	0.0	1.07	2.45	1.04	No	No
+ fences (F*)						

Notes: *U = Unfueled run, *F = Fueled run just prior to inlet unstart

Table 3. Blockage results for various test configurations ($p_{t,h}$ = 175 psia and $T_{t,h}$ = 2095°R.)

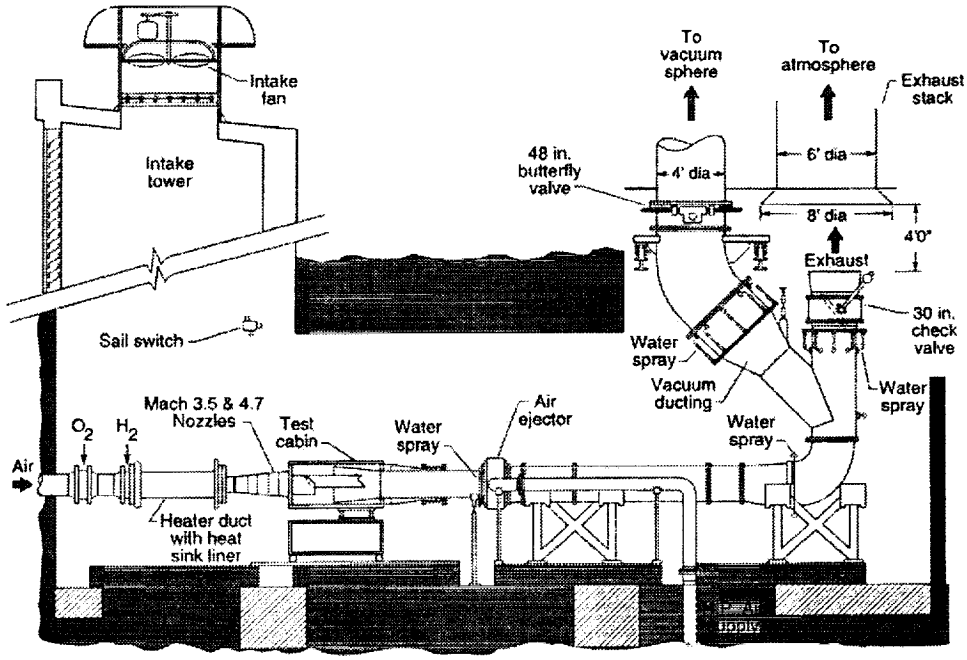

Figure 1. Schematic of the NASA Langley Combustion Heated Scramjet Test Facility. Dimensions are in feet unless stated otherwise.

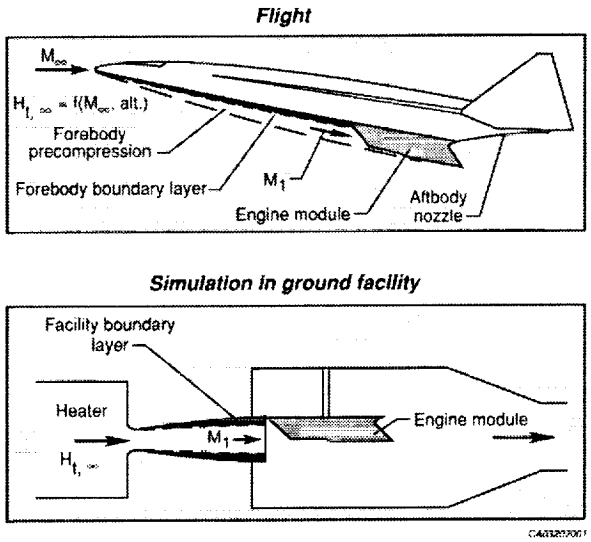

Figure 2. Matching flight conditions.

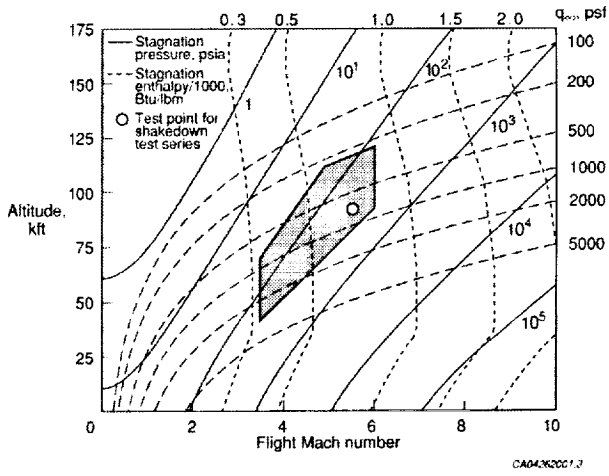

Figure 3. Flight simulation envelope for the LaRC Combustion Heated Scramjet Test Facility.

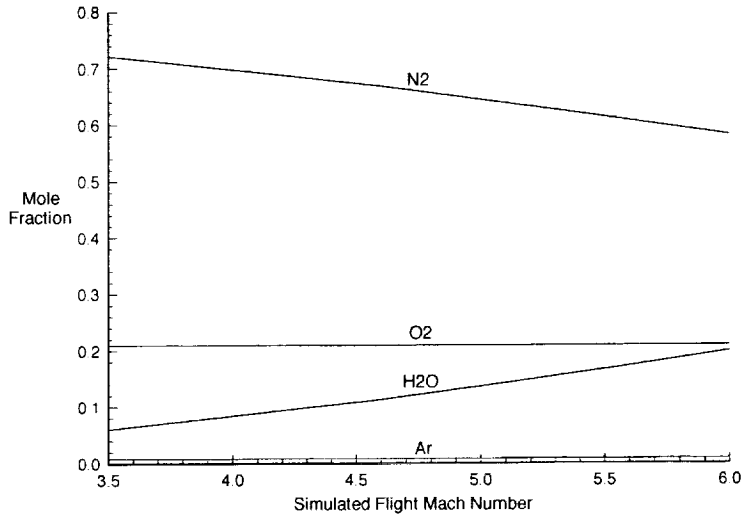

Figure 4. Test gas composition as a function of flight Mach number (q_∞ = 1000 psf)

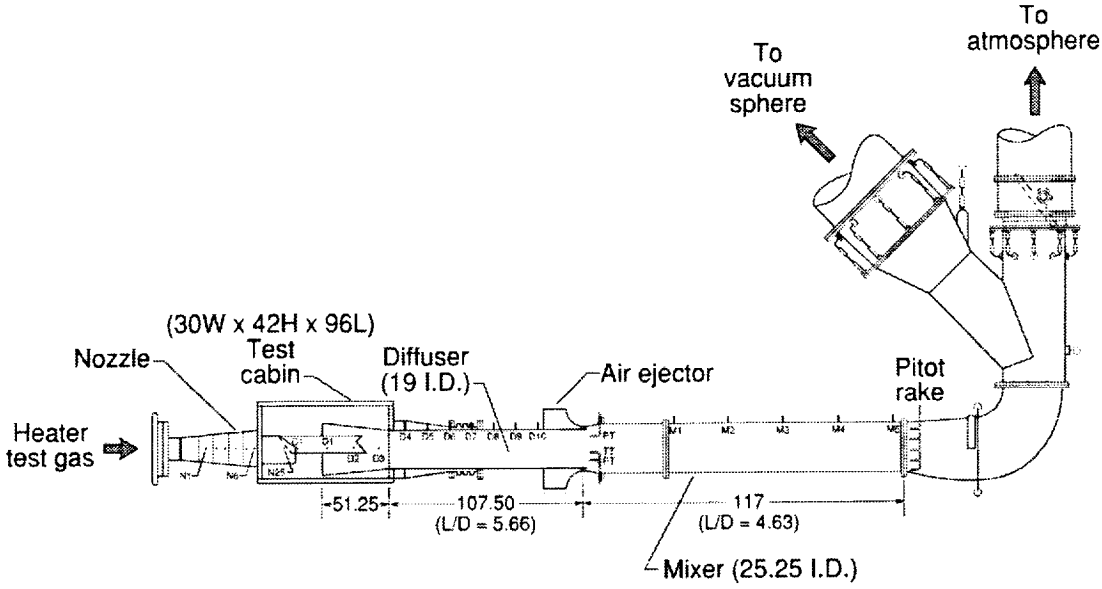

Figure 5. Current facility diffuser schematic and instrumentation. (All dimensions are in Inches.)

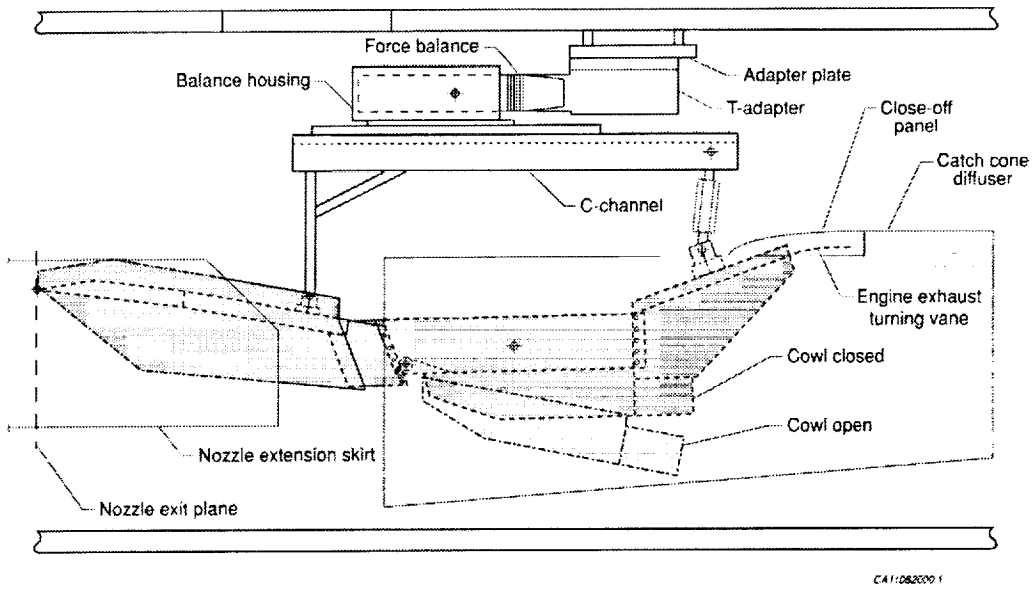

Figure 6. DFX Mach 5 engine installed in the CHSTF test cabin, Baseline configuration, y_{le} = 2.0 in.

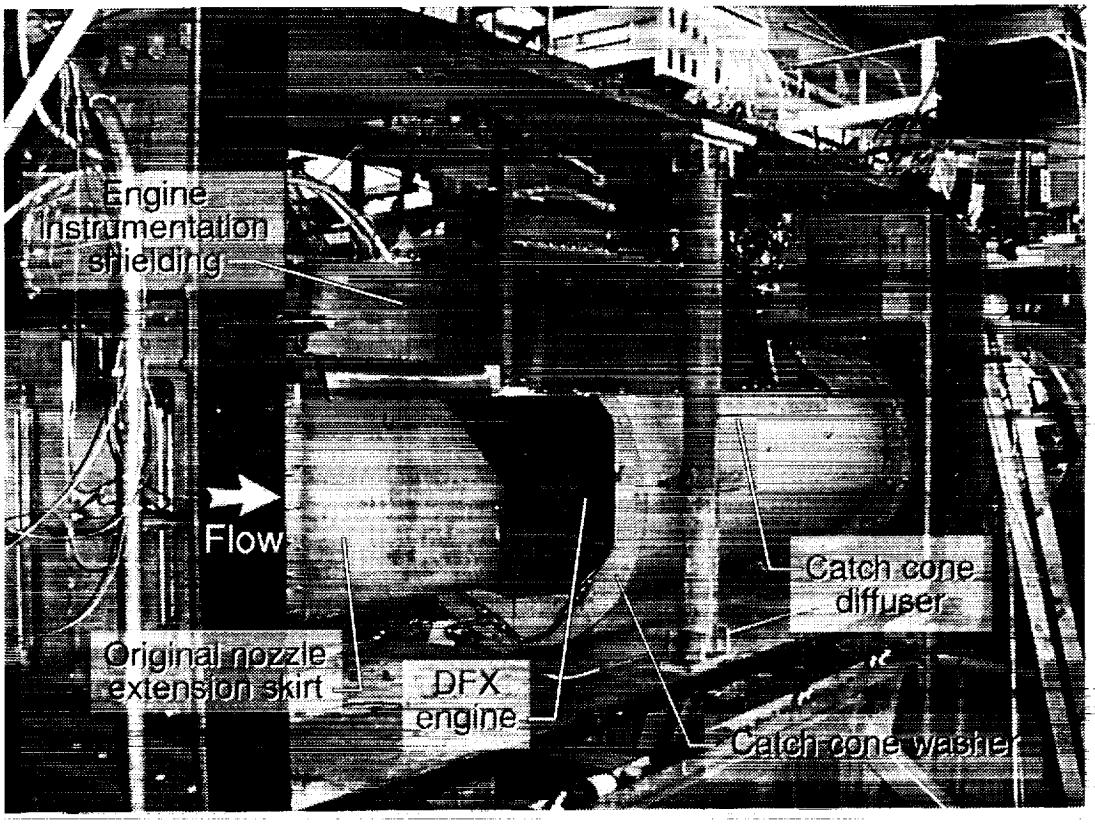

Figure 7. Photograph of the DFX installed in CHSTF test cabin (original configuration, y_{le} = 2.0 in.)

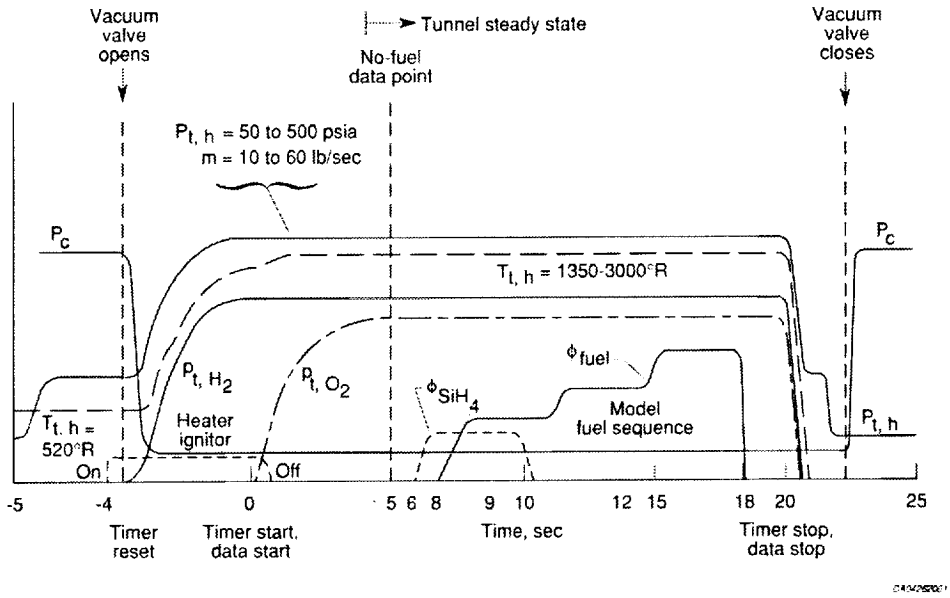

Figure 8. Typical run sequence for the Combustion Heated Scramjet Test Facility.

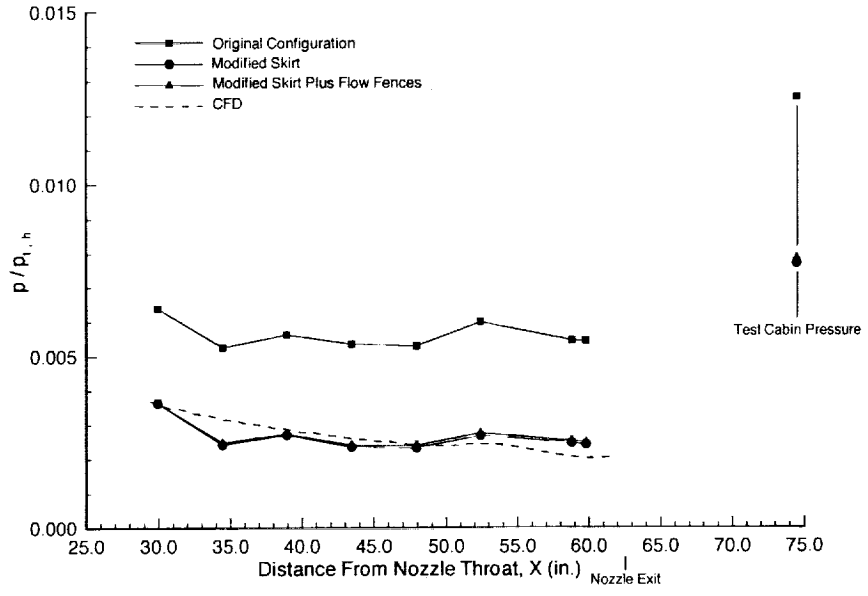

Figure 9. Static pressure distributions along the CHSTF nozzle, y_{le} = 2.0 in.

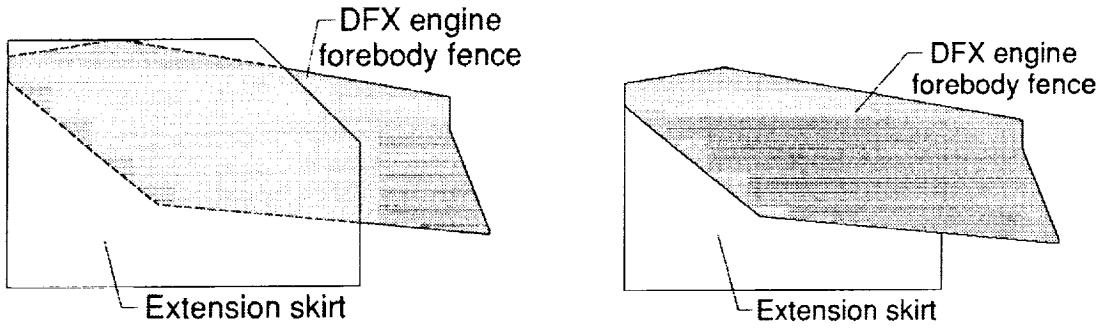

(a) Original nozzle extension skirt

(b) Modified nozzle extension skirt

Figure 10. Nozzle extension skirt modification.

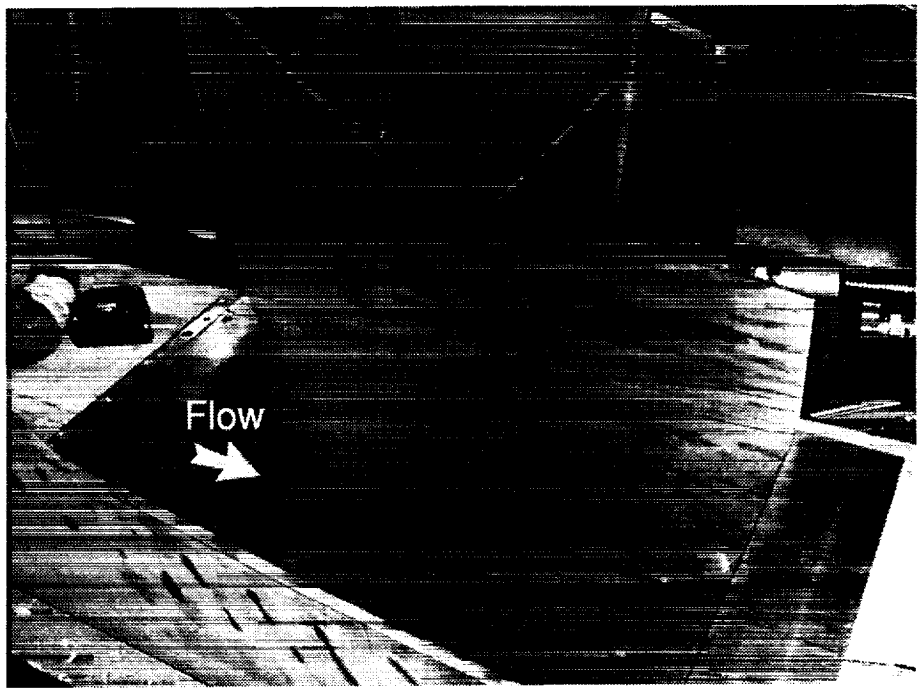

Figure 11. Oil flow patterns obtained on the modified skirt, y_{le} = 2.0 in.

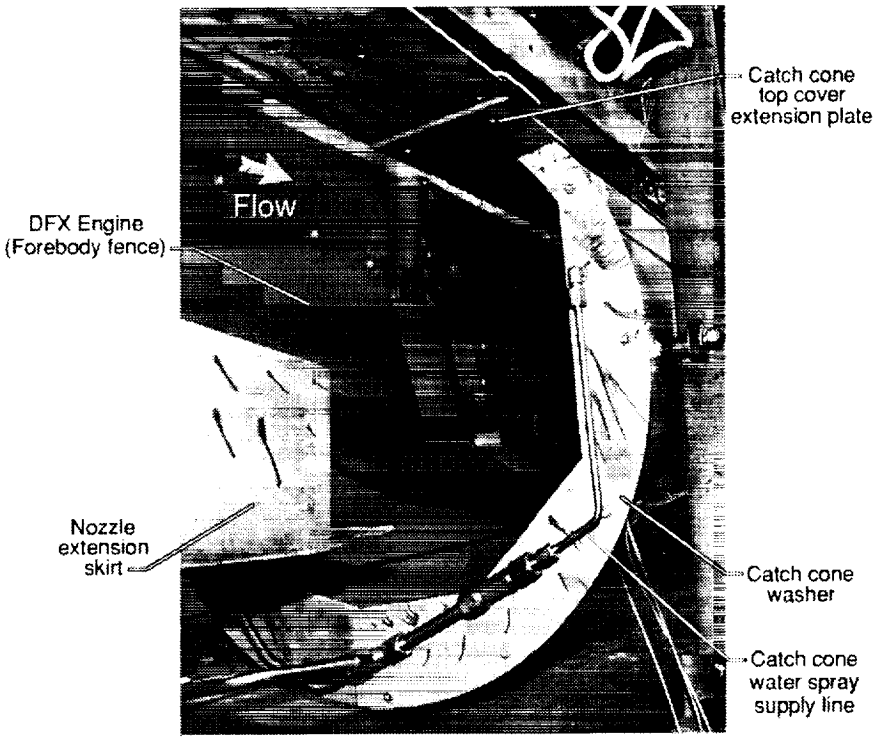

Figure 12. Oil flow patterns on the catch cone extension plate and washer (modified skirt, y_{le} = 2.0 in.)

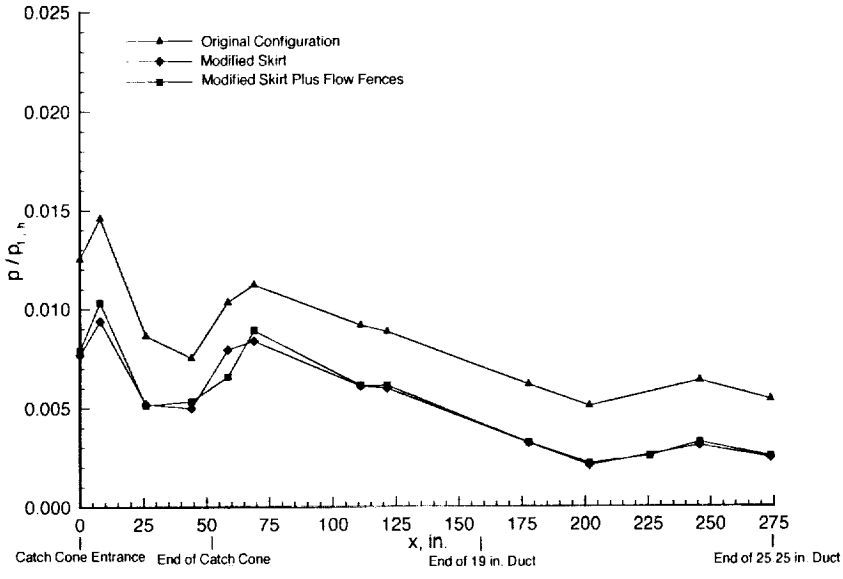

Figure 13. Static pressure distributions along the facility diffuser. (y_{le} = 2.0 in.)

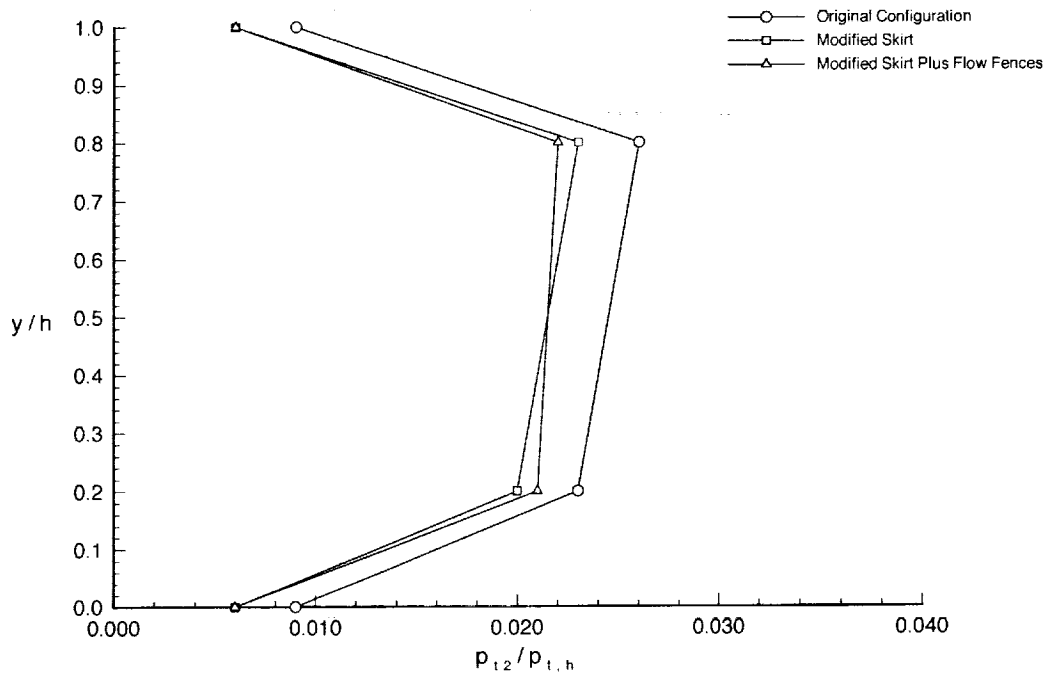

Figure 14. Pitot pressure distributions at the exit of the 19 in. I.D. diffuser (y_{le} = 2.0 in.)

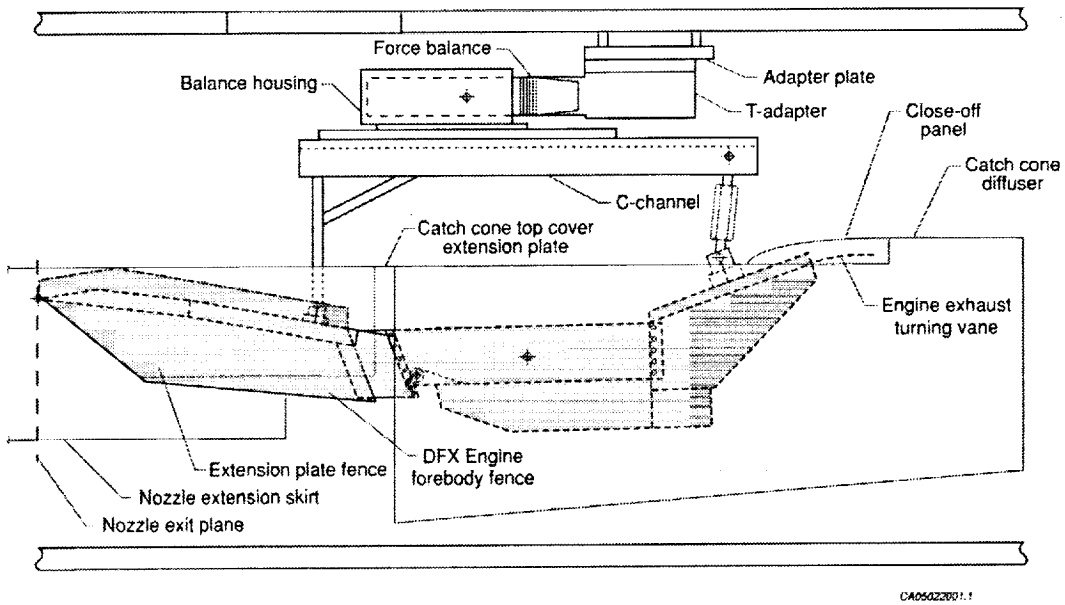

Figure 15. Aeroappliance modifications.

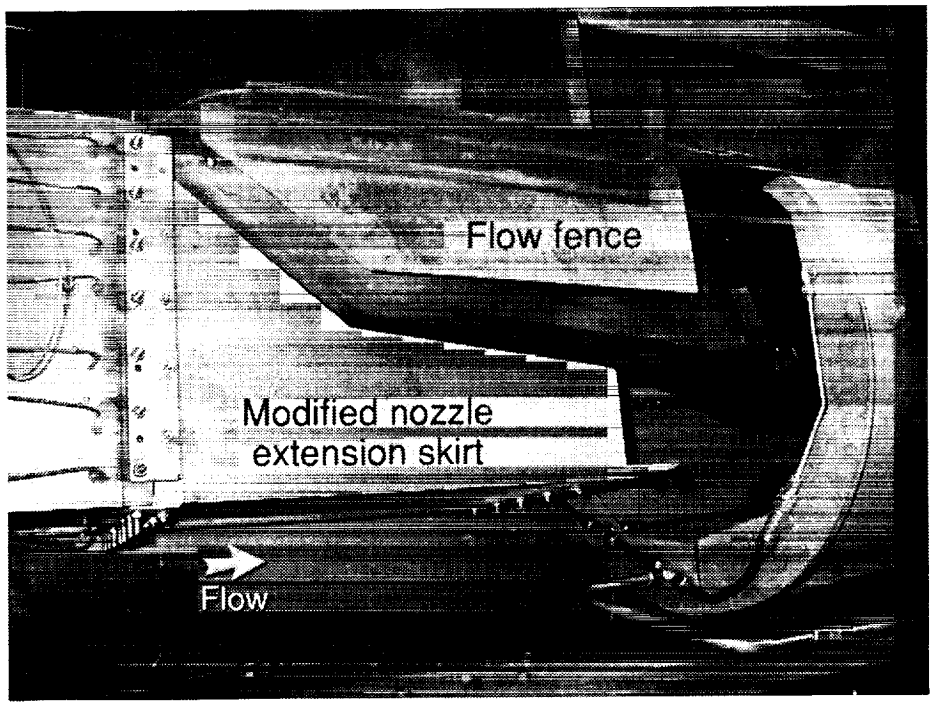

Figure 16. DFX installed in CHSTF test cabin (Modified extension skirt plus flow fences, y_{le} = 0.0 in.)

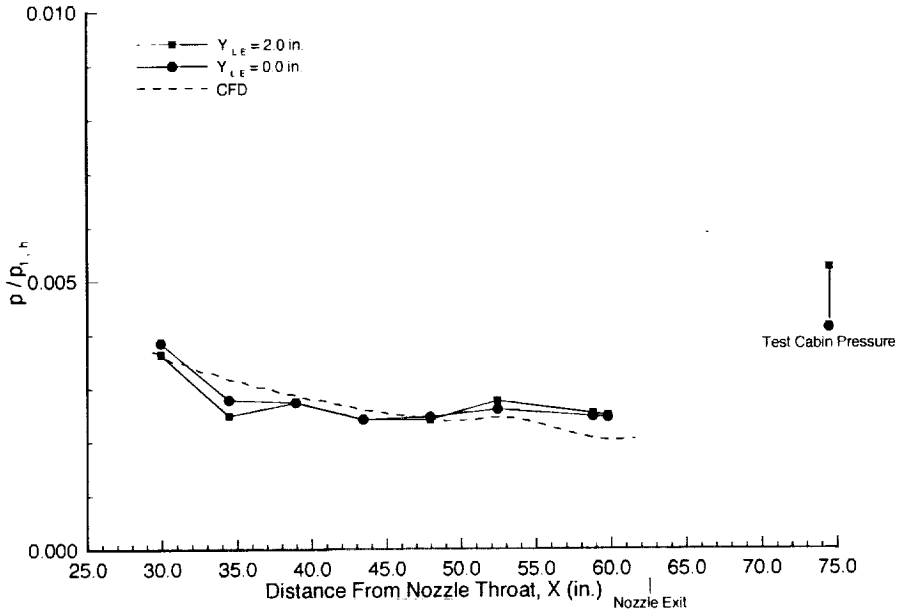

Figure 17. Static pressure distributions along the facility nozzle. (Modified extension skirt plus flow fences, y_{le} = 0.0 and 2.0 in.)

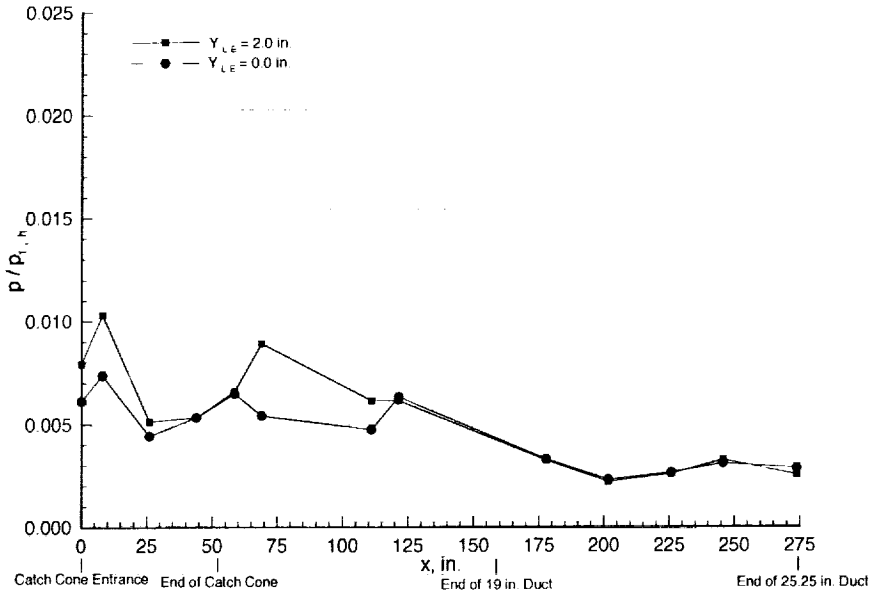

Figure 18. Static pressure distributions along the facility diffuser. (Modified extension skirt plus flow fences, y_{le} = 0.0 and 2.0 in.)

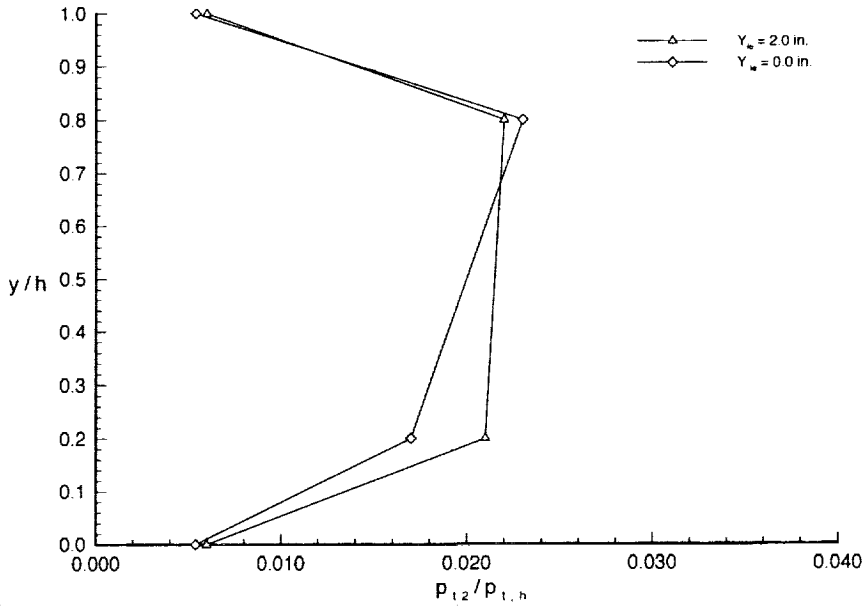

Figure 19. Pitot pressure distributions at the exit of the 19 in. I.D. diffuser (Modified extension skirt plus flow fences, y_{le} = 0.0 and 2.0 in.)

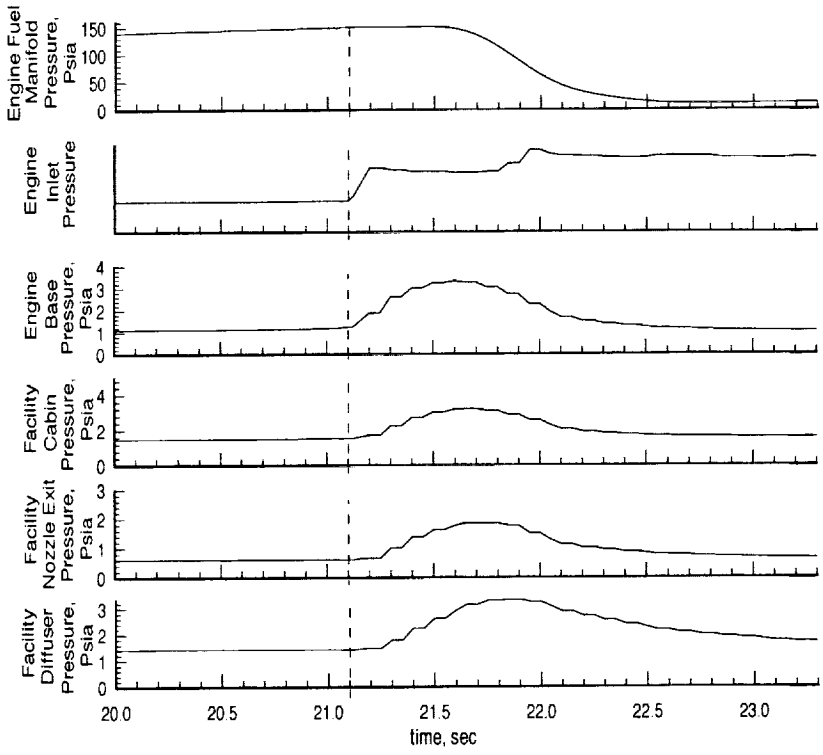

Figure 20. Time history plot showing the facility response to a DFX inlet unstart, y_{le} = 0.0 in.

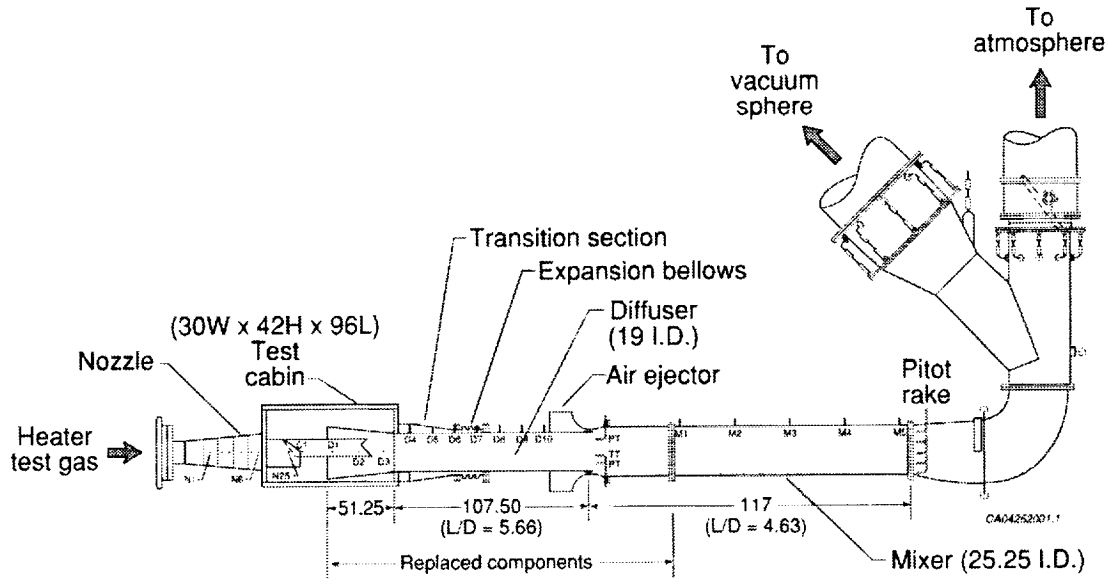

Figure 21. Schematic of original exhaust system showing components to be replaced

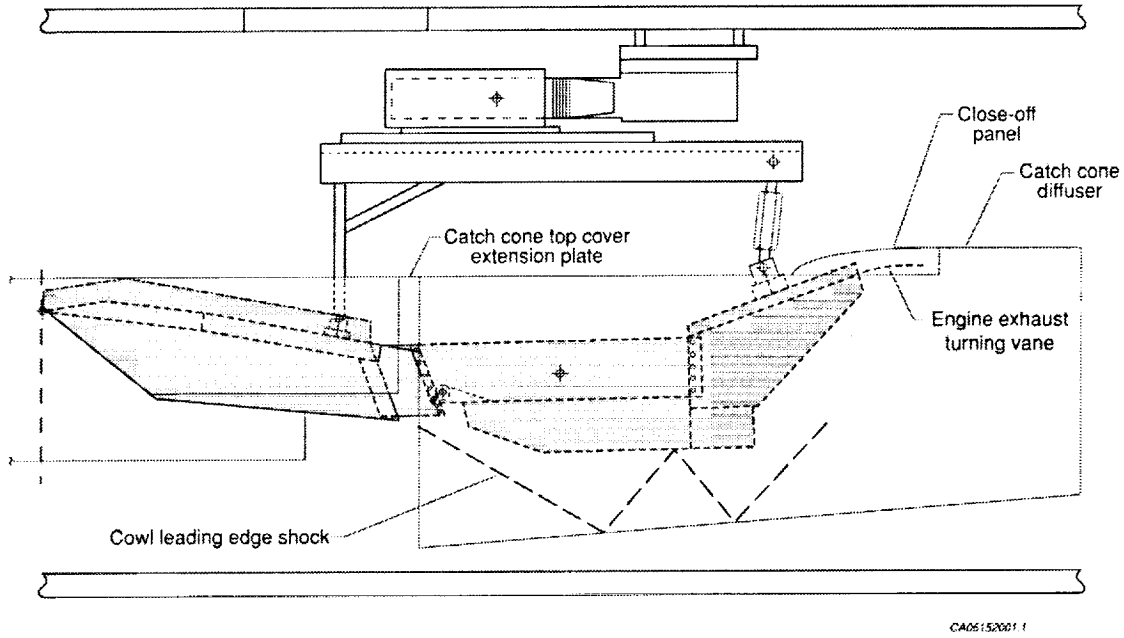

Figure 22. Cowl shock pattern within original catch cone diffuser.

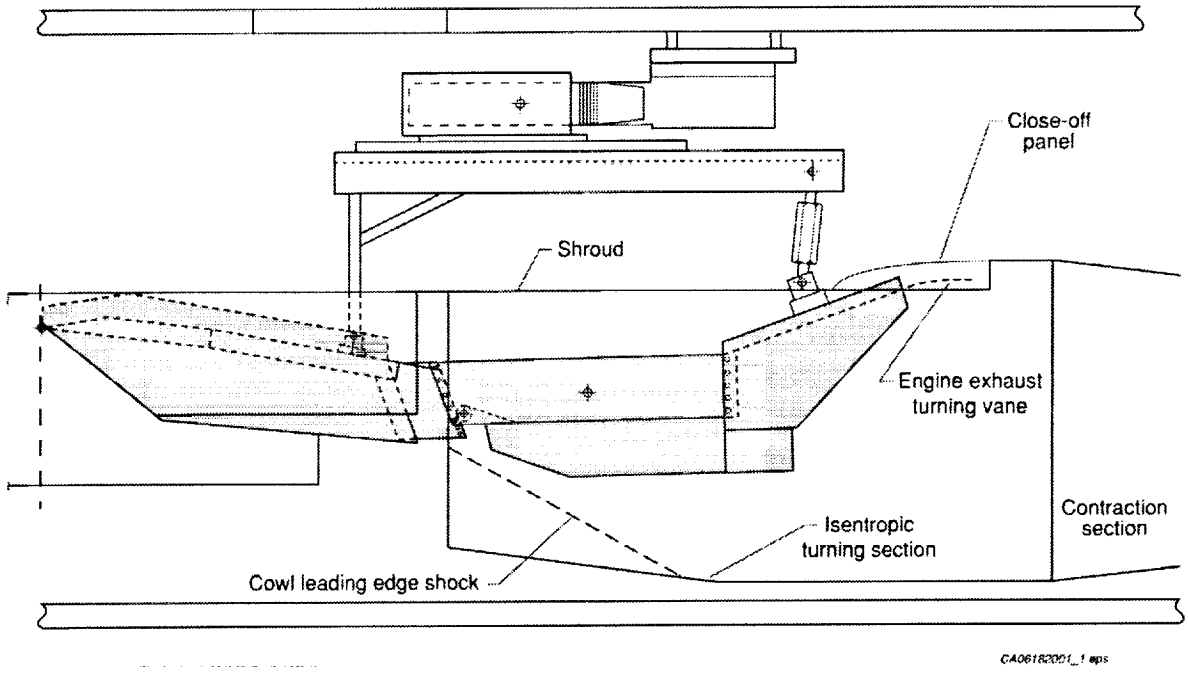

Figure 23. Cowl shock pattern within new shroud.

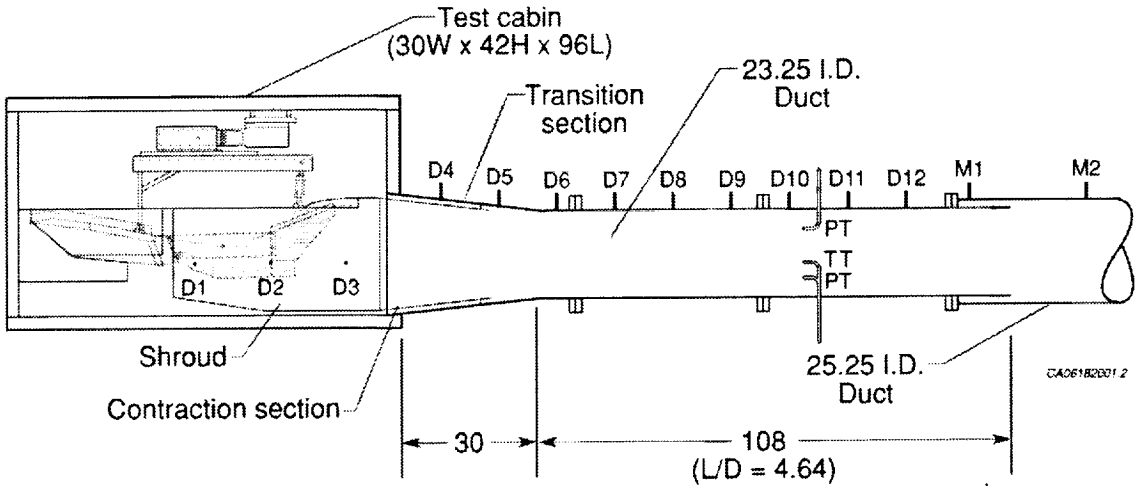

Figure 24. New shroud and facility diffuser sections.